Catalysis Letters 48 (1997) 145–150

Vanadium (V) complexes in molten salts of interest for the catalytic oxidation of sulphur dioxide

Soghomon Boghosian*, Flemming Borup and Athanassios Chrissanthopoulos

Department of Chemical Engineering, University of Patras and
Institute of Chemical Engineering and High Temperature Chemical Processes (ICE/HT-FORTH),
PO Box 1414, GR-26500 Patras, Greece
E-mail: boghosian@rea.iceht.forth.gr

Received 23 May 1997; accepted 8 September 1997

High temperature Raman spectroscopy is used for the first time for establishing the structural and vibrational properties of V^V complexes in V_2O_5–$Cs_2S_2O_7$ ($0 \leqslant X^0_{V_2O_5} \leqslant 0.24$) and V_2O_5–$Cs_2S_2O_7$–Cs_2SO_4 ($0 \leqslant X^0_{V_2O_5} \leqslant 0.25$) molten salt mixtures at 450°C under static equilibrium conditions. Based on Raman band intensity correlations and band assignments it is found that the V^V complex present in V_2O_5–$Cs_2S_2O_7$ molten mixtures has a dimeric $(VO)_2O(SO_4)_4^{4-}$ configuration containing a V–O–V bridge. Addition of Cs_2SO_4 in V_2O_5–$Cs_2S_2O_7$ mixtures results in the reaction of the V^V dimer with sulfate ions and the spectral data obtained are accounted for by the following reaction scheme: $(VO)_2O(SO_4)_4^{4-} + 2SO_4^{2-} \rightarrow 2VO_2(SO_4)_2^{3-} + S_2O_7^{2-}$. The results are of value for the progress on the mechanistic understanding of the SO_2 oxidation at the molecular level.

Keywords: vanadium (V) complexes, Raman spectroscopy, molten salt catalysts, SO_2 oxidation, sulfato complexes

1. Introduction

The catalytic oxidation of SO_2 is known to occur as a homogeneous reaction at 400–600°C in a molten phase consisting of V_2O_5 dissolved in $M_2S_2O_7$ (M = Na, K, Cs), which is dispersed on an inert support [1–3]. Despite persistent research efforts, conclusions concerning the molecular structure of the V^V and V^{IV} complexes participating in the catalytic cycle still remain to be reached [4]. Unfortunately, a direct study of the species formed in the liquid phase, which is dispersed in the small pores of the industrial catalyst, is very difficult. To date it has been impossible to undertake any high temperature vibrational spectroscopic study of *supported molten salt* catalysts, whereas only methods like ESR [3,5] and NMR [6] could be applied. The study, however, of the two-phase molten salt/gas systems V_2O_5–$M_2S_2O_7$–M_2SO_4/SO_2–O_2–SO_3–N_2 (M = K, Cs, Na or mixtures of these), which represent realistic models of the catalyst, can lead to exploration of the catalyst's chemistry. In this context, investigations based on potentiometric, cryoscopic, spectrophotometric, conductometric and calorimetric work have been undertaken to study the V^V complexes in V_2O_5–$M_2S_2O_7$–M_2SO_4 (M = K, Cs) melts [7–10]. Furthermore, the phase diagrams of the catalytically important V_2O_5–$M_2S_2O_7$ (M = 80% K + 20% Na) [11], V_2O_5–$K_2S_2O_7$ [12] and V_2O_5–$Cs_2S_2O_7$ [13] systems have been constructed. $Cs_4(VO)_2O(SO_4)_4$ is the only V^V crystalline compound isolated from V_2O_5–$M_2S_2O_7$ molten systems [14].

In a previous work [4], high temperature spectroscopic methods (UV/VIS, ESR) had been applied for the first time to study the complex formation of V^{IV} in the molten salt–gas system V_2O_5–$K_2S_2O_7$/SO_2–SO_3–N_2 under equilibrium conditions, whereas more recently NMR has been applied for the study of V_2O_5–$Cs_2S_2O_7$ melts [15]. The present article is the first report of high temperature Raman spectra obtained for the V_2O_5–$Cs_2S_2O_7$–Cs_2SO_4 melts under oxygen atmosphere which simulate the oxidised form of the Cs-promoted sulfuric acid catalyst's active molten phase. The data obtained provide conclusive evidence about the nature and the structural properties of the active V^V complexes present in this catalytically important molten salt system. The study extends in the mole fraction range $X_{V_2O_5} = 0$–0.25 (up to 6 mol V dm^{-3}) at 450°C, thus covering the catalyst composition (usually in the range $X_{V_2O_5} = 0.18$–0.22 (up to 5 mol V dm^{-3})). The vibrational frequencies of the complexes formed in the molten state were determined and the data are discussed in terms of possible structures.

2. Experimental

2.1. Sample preparation

The samples were prepared by mixing V_2O_5 (Cerac, Pure 99.9%), $Cs_2S_2O_7$ (made by thermal decomposition of $Cs_2S_2O_8$, which was synthesised in the laboratory as described previously [16]) and Cs_2SO_4 (Fluka) which was dried by heating in vacuo at 300°C for 4 h. All handling of chemicals and filling of the Raman optical cells (made of cylindrical fused silica tubing (4 ± 0.1 mm o.d.,

---

[*] To whom correspondence should be addressed.

2 ± 0.1 mm i.d. and ~3 cm long for the part containing the molten salts)) took place in a nitrogen-filled glove box. The symbol X_i^0 is used to denote the mole fractions of nonreacted components of the V_2O_5–$Cs_2S_2O_7$ binary mixture (weighed-in amounts) before the addition of Cs_2SO_4. The samples were sealed under a low pressure (ca. 0.2 atm) of O_2 (L'Air Liquide, 99.99%) in order to stabilise vanadium in the pentavalent state and were equilibrated at 450°C for up to 20 days before recording the Raman spectra. The long equilibration time was particularly necessary for the ternary V_2O_5–$Cs_2S_2O_7$–Cs_2SO_4 mixtures due to the slow dissolution of sulfate.

2.2. High temperature Raman spectra

Raman spectra were excited with the 647.1 and 676.4 nm lines of a Spectra Physics Stabilite model 2017 krypton ion laser. The experimental set-up used and the procedures followed for obtaining Raman spectra at high temperatures have been described in detail elsewhere [17]. It should be pointed out here that recording of the Raman spectra at elevated temperatures from these very dark-coloured, viscous and hygroscopic melts has proven very difficult due to strong absorption of the incident exciting laser light.

During the present investigation, the optical geometry, the spectral slit width and the laser power measured before and after the entrance and exit windows of the furnace were maintained constant. The Raman cells were placed inside the mechanically stable metal core of the furnace and were always in a fixed position relative to the collecting lens and entrance slit. The intensity of the scattered light was maximized by positioning the focusing and collecting lenses with two x,y,z microposi-

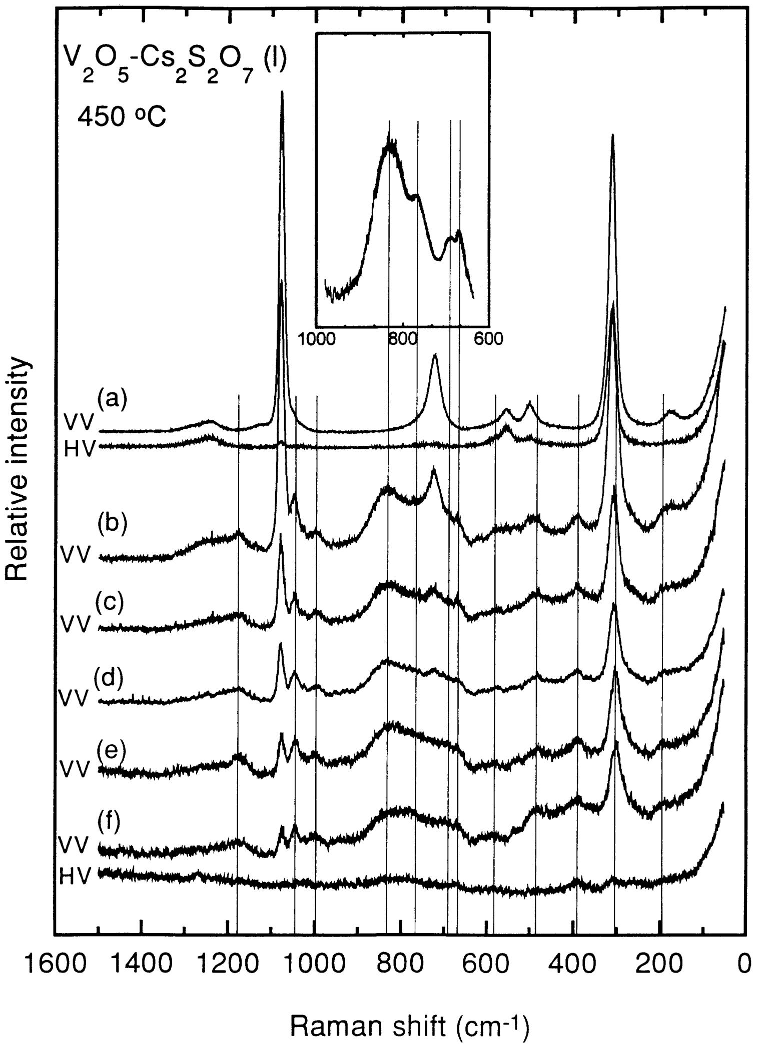

Figure 1. Raman spectra of the V_2O_5–$Cs_2S_2O_7$ molten mixtures at 450°C; (a): $X^0_{V_2O_5} = 0$ at 470°C; (b): $X^0_{V_2O_5} = 0.065$; (c): $X^0_{V_2O_5} = 0.106$; (d): $X^0_{V_2O_5} = 0.146$; (e): $X^0_{V_2O_5} = 0.206$; and (f): $X^0_{V_2O_5} = 0.241$. Bands due to the $(VO)_2O(SO_4)_4^{4-}$ (l) complex are marked by vertical lines. $\lambda_0 = 647.1$ nm; laser power, $w = 175$ mW; scan rate, sr, 60 cm^{-1} min^{-1} for (a)–(d), 18 cm^{-1} min^{-1} for (e)–(f); time constant, τ, 0.3 s for (a), 1 s for (b)–(d), 3 s for (e)–(f); spectral slit width, sww, 7 cm^{-1}. VV and HV denote the vertical–vertical and horizontal–vertical spectra polarizations, respectively. Insert: region of spectrum (b) after subtraction of the 725 cm^{-1} $S_2O_7^{2-}$ band.

tioners. After obtaining the spectra the cell could be removed and cooled to room temperature and then reintroduced into the optical furnace, yielding always with no further micropositioner adjustments the same Raman intensities. Thus, by the use of the same experimental conditions the Raman intensities could be reproduced to within 2–5%.

3. Results and discussion

Several V_2O_5–$Cs_2S_2O_7$ mixtures with compositions $X^0_{V_2O_5} = 0$–0.24 were placed in cells. Upon dissolution of V_2O_5 in the pyrosulfate solvent at 450°C, dark brown melts were obtained and recording of Raman spectra for melts with $X^0_{V_2O_5} \geqslant 0.2$ was extremely difficult due to very strong absorption of the excitation laser lines used. Figure 1 shows Raman spectra of V_2O_5–$Cs_2S_2O_7$ molten mixtures obtained at 450°C for five different compositions (figure 1 (b)–(f)). The Raman spectra of pure molten caesium pyrosulfate were also recorded and are included in figure 1 (a) for comparison. The strongest band of the $S_2O_7^{2-}$ ion in molten $Cs_2S_2O_7$ is at 1078 cm^{-1}. Addition of V_2O_5 gives rise to the appearance of several new bands (i.e. other than the ones due to $Cs_2S_2O_7$(l)). The most prominent new features are at 1176, 1047 (due to V=O terminal stretching), 996, 839, 765, 670/690, 582, 486, 393, 302 and 196 cm^{-1} and are indicated in figure 1 by vertical lines. The existence of the 765 and 670/690 cm^{-1} bands is better illustrated in figure 1 (insert) where the contribution of the 725 cm^{-1} $S_2O_7^{2-}$ band is subtracted from the 600–1000 cm^{-1} region of spectrum (b). The intensities of all the above new bands increase relative to the bands of the $S_2O_7^{2-}$ ion with increasing $X^0_{V_2O_5}$ and dominate the spectra (e) and (f) of the samples with $X^0_{V_2O_5} = 0.206$ and $X^0_{V_2O_5} = 0.241$ indicating that the reaction taking place leads to a vanadium oxo sulfato complex at the expense of the $S_2O_7^{2-}$ ion as illustrated also in figure 2. By plotting (see figure 2A) the quantity $I^* = [I(S_2O_7^{2-}, 1078)/X^0_{S_2O_7}]/[I(V{=}O, 1047)/X^0_{V_2O_5}]$ vs. $X^0_{V_2O_5}$ – where $I(S_2O_7^{2-}, 1078)$ and $I(V{=}O, 1047)$ are the relative intensities due to the $\nu_1(S_2O_7^{2-})$ and V=O stretching modes in each composition and X^0_i are the initial mole fractions (weighed-in amounts) – it becomes evident by extrapolation that within the experimental error there would be no $S_2O_7^{2-}$ left for $X^0_{V_2O_5} = 0.33$. Furthermore, by considering the general complex formation scheme

$$V_2O_5 + nS_2O_7^{2-} \rightarrow C^{2n-} \qquad (1)$$

one is able to calculate the equilibrium mole fractions X_{eq,S_2O_7} and $X_{eq,C}$ by the following mole balance equations:

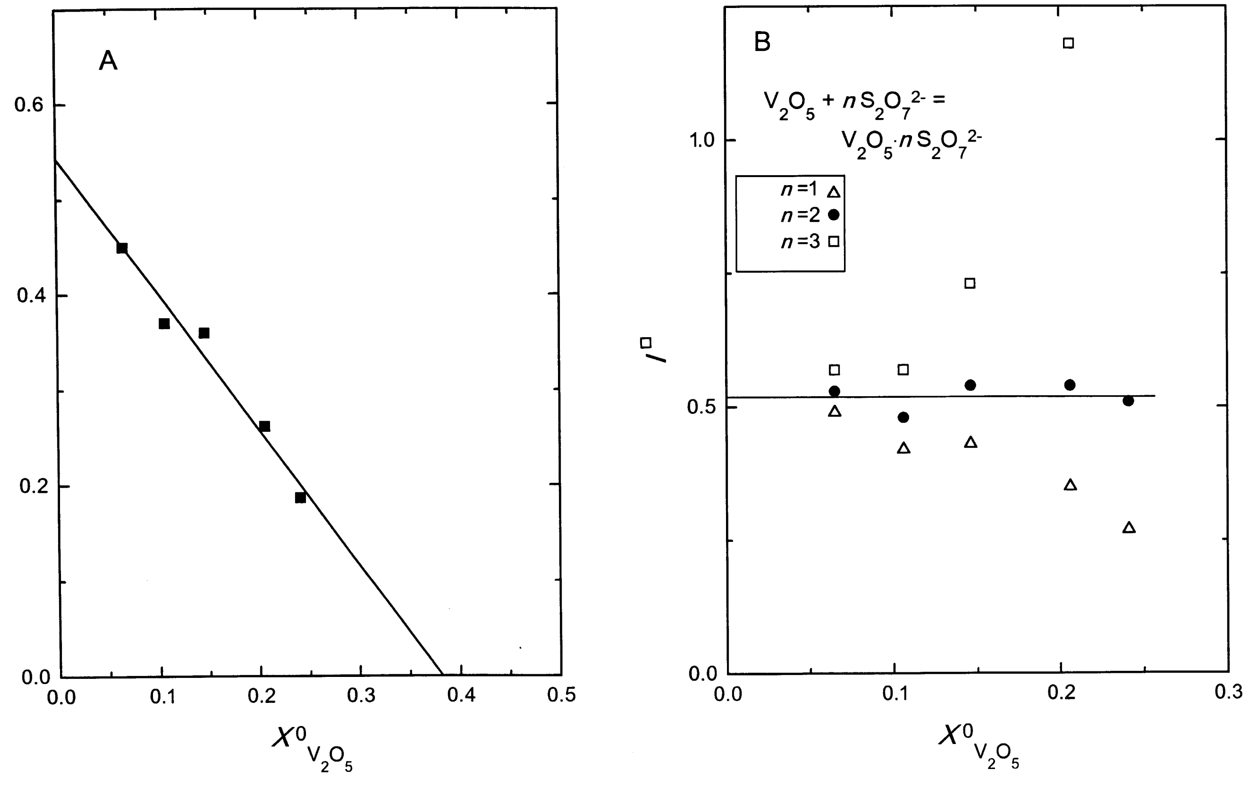

Figure 2. (A) Plot of $I^* = [I(S_2O_7^{2-}, 1078)/X^0_{S_2O_7}]/[I(V{=}O, 1047)/X^0_{V_2O_5}]$ vs. $X^0_{V_2O_5}$ for the five compositions studied (see text). (B) Plots of $I^\square = [I(S_2O_7^{2-})/X_{eq,S_2O_7}]/[I(C)/X_{eq,C}]$ vs. $X^0_{V_2O_5}$ for the five compositions studied, calculated for $n = 1$ (△), $n = 2$ (●) and $n = 3$ (□).

$$X_{eq,S_2O_7} = (N^0_{S_2O_7} - nN^0_{V_2O_5}) \Big/ \left(\sum N^0_i - nN^0_{V_2O_5}\right)$$

and

$$X_{eq,C} = N^0_{V_2O_5} \Big/ \left(\sum N^0_i - nN^0_{V_2O_5}\right).$$

It then follows that for a correct choice of n the quantity $I^{\square} = [I(S_2O_7^{2-})/X_{eq,S_2O_7}]/[I(C)/X_{eq,C}]$ should have a constant value independent on melt composition. In fact, $I^{\square}$ corresponds to the intensity ratio of one $S_2O_7^{2-}$ ion relative to one complex ion. The plot in figure 2B indeed confirms that the correct stoichiometry is reflected by $n = 2$ as shown by the horizontal line from which the $I^{\square}$ values for $n = 1$ and $n = 3$ depart significantly. The $Cs_2S_2O_7$–V_2O_5 phase diagram indicates a compound melting at 412°C at a composition corresponding to $2Cs_2S_2O_7 \cdot V_2O_5$ [16]. By taking also into account the earlier NMR evidence [15] suggesting the existence of a *dimeric* V^V complex furthermore strengthened by the fact that the only crystalline V^V compound isolated so far from V_2O_5–$Cs_2S_2O_7$ molten mixtures is the $Cs_4(VO)_2O(SO_4)_4$ [14], it follows that the reaction taking place can be formulated only as

$$V_2O_5 + 2S_2O_7^{2-} \rightarrow (VO)_2O(SO_4)_4^{4-} \qquad (2)$$

Within the $Cs_4(VO)_2O(SO_4)_4$ compound there are four crystallographically different bidentate chelating significantly distorted sulfate groups with S–O bonds having largely varying distances [14]. The terminal S–O bonds are in the range 1.43–1.44 Å while the S–O bonds involving oxygen coordinated to vanadium (bridging S–O bonds) are *unusually* long ranging between 1.52 and 1.58 Å, far from the usual value of 1.47 Å found for the ideal sulfate group. Furthermore, a value of 961 cm^{-1} is found for the $\nu_1(SO_4^{2-})$ mode of free sulfate in $Cs_2S_2O_7$–Cs_2SO_4 melts (see figure 3 (a)). It is therefore evident that, if the $(VO)_2O(SO_4)_4^{4-}$ ion is the dimer complex formed in the molten state, then one could assign the 996 cm^{-1} band to the short terminal S–O stretching mode (S–O$_t$) and the 839 cm^{-1} broad feature to the long bridging S–O modes (S–O$_b$). The above variation in sulphur–oxygen stretching frequencies is compatible with the departures from the 1.47 Å ideal S–O bond length and is analogous to the differences observed between terminal and bridging metal–halogen stretching frequencies [18]. The 1176 cm^{-1} band is identified as the $\nu_3(SO_4^{2-})$ mode and the 670/690 cm^{-1} doublet can be assigned to $\nu_4(SO_4^{2-})$. The 1047 cm^{-1} is assigned to the V^V=O terminal mode in agreement with what would be expected [18], while the 765, 582 and 486 cm^{-1} bands are assigned to V–O bridging. In particular, the 765 cm^{-1} band is assigned to the V–O–V bridging mode of the dimer $(VO)_2O(SO_4)_4^{4-}$ complex and the 582, 486 cm^{-1} bands can be due to V–O bridging involving sulfate oxygen (along the –V–O–S– chains). Such an assignment for these bands is in agreement with the relative V–O distances along the –V–O–V– and –V–O–S– chains within the $Cs_4(VO)_2O(SO_4)_4$ compound [14] and with a correlation between V–O Raman stretching frequencies and bond lengths [19]. Naturally, the band assignments for such complex species can be open to long discussion which, however, is beyond the scope of the present article.

A closer inspection of the spectral series in figure 1 reveals that while in spectrum (b) the bands in the 650–690 cm^{-1} range are well resolved (see insert in figure 1), the same bands appear to broaden and overlap each other with increasing V_2O_5 mole fraction. This is caused most probably due to polymerization of the V^V dimer complex as indicated by the significant increase in the melt viscosity and suggested also by NMR [15]. It is evident that polymerization of the $(VO)_2O(SO_4)_4^{4-}$ complex would lead to several related configurations of bridging S–O–V and V–O–V bands, a fact which explains the observed band broadening and the apparent band shifts in the 650–690 cm^{-1} region. It is more clear that bands due to terminal modes (e.g., at 996 and 1047 cm^{-1}) are affected much less from the polymerization.

Addition of Cs_2SO_4 to V_2O_5–$Cs_2S_2O_7$ melts results in reactions with the $(VO)_2O(SO_4)_4^{4-}$ complex. The reaction was followed by recording Raman spectra at 450°C for a V_2O_5–$Cs_2S_2O_7$ sample with fixed $X^0_{V_2O_5}$ in which various amounts of Cs_2SO_4 were added. A titration-like series of Raman spectra was thus obtained, which indicates that the V^V dimer ($(VO)_2O(SO_4)_4^{4-}$) reacts with the added sulfate up to a SO_4^{2-}/V^V ratio (ratio of number of added sulfate moles reacting vs. number of extant V^V atoms) equal to 1. Figure 3 (a)–(c) shows Raman spectra of V_2O_5–$Cs_2S_2O_7$ melts with $X^0_{V_2O_5} = 0.027$–0.147 saturated with Cs_2SO_4. The band at 961 cm^{-1} in spectrum 2 (a) is due to the ν_1 mode of dissolved free SO_4^{2-}. The band at 941 cm^{-1} is due to coordinated sulfate and its relative intensity increases with increasing content of V_2O_5 (see, e.g., spectra (b)–(c)). Furthermore, a comparison of spectrum 1 (d) with 3 (c) from samples with the same initial $X^0_{V_2O_5} = 0.15$ shows that reaction with Cs_2SO_4 results in elimination of the 996 (S–O$_t$), 839 (S–O$_b$), 765 (V–O–V) and 302 cm^{-1} bands, appearance of a new S–O stretching mode at 941 cm^{-1} and small shifts of the V^V=O to 1038, of the V–O–S to 666 and of the $\nu_3(SO_4^{2-})$ mode to 1166 cm^{-1}. Finally a low frequency doublet at 226/279 cm^{-1} also appears. Thus, addition of Cs_2SO_4 results in cleavage of the V–O–V bridge and in formation of a V^V complex which contains coordinated sulfate groups exhibiting smaller distortions to their symmetry as judged from the departure of the S–O stretching frequency from the 961 cm^{-1} "ideal" value.

In order to examine the reaction of molten $Cs_4(VO)_2O(SO_4)_4$ with caesium sulfate the following procedure was adopted. The compound $Cs_4(VO)_2O(SO_4)_4$ was synthesised by slow cooling of a V_2O_5–$Cs_2S_2O_7$ molten mixture with $X^0_{V_2O_5} = 0.33$; it was afterwards mixed with excess Cs_2SO_4 and equilibrated at

450°C. The Raman spectrum of the resulting melt is depicted in figure 3 (d) and shows that the reaction proceeds with the formation of $S_2O_7^{2-}$ as indicated by the presence of the characteristic (see figure 1 (a)) 1078, 725 and 313 cm^{-1} bands. The above observations of (i) a 1 : 1 SO_4^{2-}/V^V ratio of number of added sulfate moles reacting vs. number of V^V atoms, (ii) cleavage of the V–O–V bridge and production of $S_2O_7^{2-}$ upon sulfate addition are accounted for by the following reaction scheme:

$$(VO)_2O(SO_4)_4^{4-} + 2SO_4^{2-} \rightarrow 2VO_2(SO_4)_2^{3-} + S_2O_7^{2-} \quad (3)$$

Eqs. (2) and (3) indicate that if all the conclusions reached and the hypotheses made up to now are correct, the constituents of a $V_2O_5{\cdot}Cs_2S_2O_7{\cdot}2Cs_2SO_4$ molten mixture would react at 450°C *stoichiometrically* to produce the $Cs_3VO_2(SO_4)_2$ molten complex without leaving excess solids or pyrosulfate ions. This is indeed the case and the Raman spectrum of the resulting $Cs_3VO_2(SO_4)_2$ molten complex is shown in figure 3 (e). From a structural point of view, the $VO_2(SO_4)_2^{3-}$ complex can be formulated from the dioxovanadium ion and two bidentate chelating sulfate groups so as to satisfy the preferential six-fold coordination for the vanadium atom and could occur as a monomer in dilute systems or as a $(VO_2(SO_4)_2)_n^{3n-}$ polymer in concentrated melts possessing one bidentate chelating and one bidentate bridging sulfate per monomer unit [8].

4. Conclusions

High temperature Raman spectra have been obtained from V_2O_5–$Cs_2S_2O_7$ ($0 \leqslant X^0_{V_2O_5} \leqslant 0.24$) and V_2O_5–$Cs_2S_2O_7$–Cs_2SO_4 ($0 \leqslant X^0_{V_2O_5} \leqslant 0.25$) molten salt mixtures

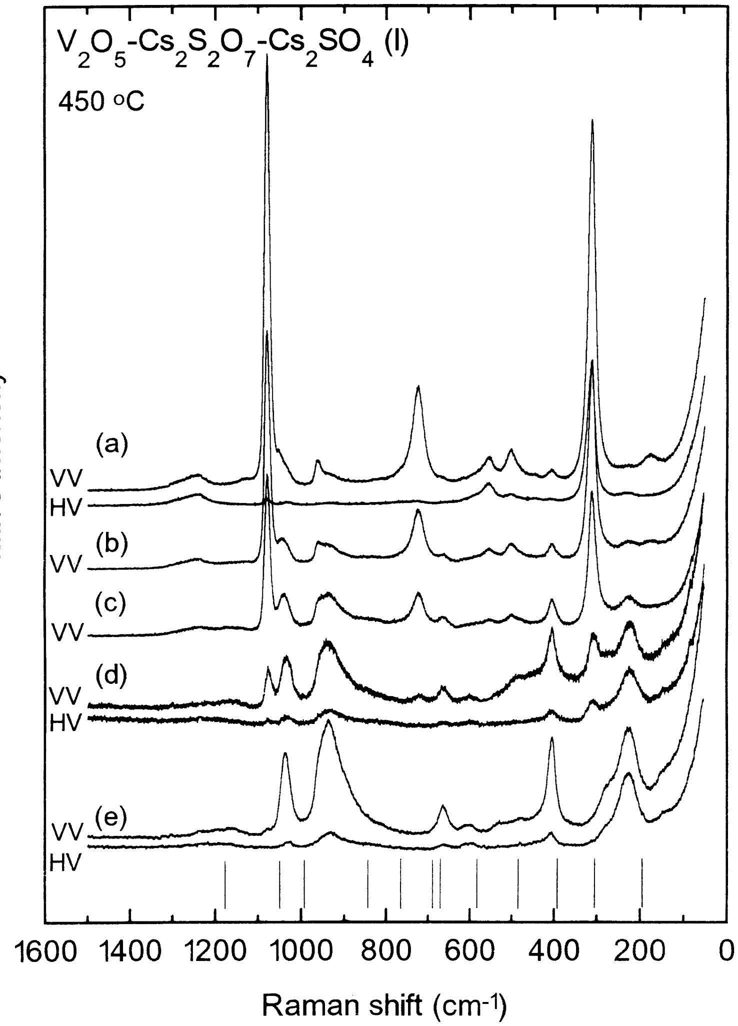

Figure 3. (a)–(c): Raman spectra of the V_2O_5–$Cs_2S_2O_7$ molten mixtures saturated with Cs_2SO_4 at 450°C; (a): $X^0_{V_2O_5} = 0.027$; (b): $X^0_{V_2O_5} = 0.066$; (c): $X^0_{V_2O_5} = 0.147$. $X^0_{V_2O_5}$ is the mole fraction of V_2O_5 in the V_2O_5–$Cs_2S_2O_7$ mixture before addition of Cs_2SO_4. (d): Raman spectrum of molten $Cs_4(VO)_2O(SO_4)_4$ saturated with Cs_2SO_4. (e): Raman spectra of the $V_2O_5{\cdot}Cs_2S_2O_7{\cdot}2Cs_2SO_4$ molten mixture at 450°C. The vertical lines mark the band positions due to the $(VO)_2O(SO_4)_4^{4-}$ (l) dimer complex which is no longer present. $\lambda_0 = 647.1$ nm; laser power, $w = 175$ mW; scan rate, sr, 90 cm^{-1} min^{-1} for (a)–(c), 30 cm^{-1} min^{-1} for (d), 60 cm^{-1} min^{-1} for (e); time constant, τ, 0.3 s for (a)–(c), 1 s for (d)–(e); spectral slit width, sww, 7 cm^{-1}.

at 450°C. It is concluded that the V^V complex present in V_2O_5–$Cs_2S_2O_7$ molten mixtures has a dimeric $(VO)_2O(SO_4)_4^{4-}$ configuration containing a V–O–V bridge with characteristic bands at 1047 (ν(V=*O*)), 996 (ν(S–O_t)), 839 (ν(S–O_b)) and 765 (ν(V–O–V)) cm^{-1}. It is found that when Cs_2SO_4 is added in V_2O_5–$Cs_2S_2O_7$ mixtures, cleavage of the V– O–V bridge occurs and the V^V dimer reacts with sulfate ions following the reaction scheme: $(VO)_2O(SO_4)_4^{4-} + 2SO_4^{2-} \rightarrow 2VO_2(SO_4)_2^{3-} + S_2O_7^{2-}$. The most characteristic bands due to the molten $VO_2(SO_4)_2^{3-}$ complex occur at 1038 (ν(V=O)) and 941 (ν(S–O_t)) cm^{-1}.

This is the first time that high temperature vibrational spectroscopy provides information on the structural properties of V^V complexes present in model melts of the sulphuric acid catalyst. The results are considered important for the progress on the mechanistic understanding of the SO_2 oxidation at the molecular level [20].

Acknowledgement

This work has been supported by the EU BRITE-EURAM II (contract BRE2.CT93.0447) Programme. Many thanks to Professor R. Fehrmann (DTU, Lyngby, Denmark) for inspiring discussions during the course of the investigation. The authors are indebted also to Professor G.N. Papatheodorou for many valuable comments and helpful discussions.

References

[1] J. Villadsen and H. Livbjerg, Catal. Rev. Sci. Eng. 17 (1978) 203.
[2] H.F.A. Topsøe and A. Nielsen, Trans. Danish Acad. Techn. Sci. 1 (1947) 3, 18.
[3] K.M. Eriksen, D.A. Karydis, S. Boghosian and R. Fehrmann, J. Catal. 155 (1995) 32.
[4] D.A. Karydis, K.M. Eriksen, R. Fehrmann and S. Boghosian, J. Chem. Soc. Dalton Trans. (1994) 2151.
[5] S.G. Masters, A. Chrissanthopoulos, K.M. Eriksen, S. Boghosian and R. Fehrmann, J. Catal. 166 (1997) 16.
[6] V.M. Mastikhin, O.B. Lapina, B.S. Bal'zhinimaev, L.G. Simonova, L.M. Karnatovskaya and A.A. Ivanov, J. Catal. 103 (1987) 160.
[7] N.H. Hansen, R. Fehrmann and N.J. Bjerrum, Inorg. Chem. 21 (1982) 744.
[8] R. Fehrmann, M. Gaune-Escard and N.J. Bjerrum, Inorg. Chem. 25 (1986) 1132.
[9] G. Hatem, R. Fehrmann, M. Gaune-Escard and N.J. Bjerrum, J. Phys. Chem. 91 (1987) 195.
[10] G. Folkmann, G. Hatem, R. Fehrmann, M. Gaune-Escard and N.J. Bjerrum, Inorg. Chem. 32 (1993) 1559.
[11] D.A. Karydis, S. Boghosian and R. Fehrmann, J. Catal. 145 (1994) 312.
[12] G. Hatem, K.M. Eriksen, M. Gaune-Escard and R. Fehrmann, J. Phys. Chem., in press.
[13] G. Folkmann, G. Hatem, R. Fehrmann, M. Gaune-Escard and N.J. Bjerrum, Inorg. Chem. 30 (1991) 4057.
[14] K. Nielsen, R. Fehrmann and K.M. Eriksen, Inorg. Chem. 32 (1993) 4825.
[15] O.B. Lapina, V.M. Mastikhin, A.A. Shubin, K.M. Eriksen and R. Fehrmann, J. Mol. Catal. A 99 (1995) 123.
[16] G. Folkmann, G. Hatem, R. Fehrmann, M. Gaune-Escard and N.J. Bjerrum, Inorg. Chem. 30 (1991) 4057.
[17] S. Boghosian and G.N. Papatheodorou, J. Phys. Chem. 93 (1989) 415, and references therein.
[18] K. Nakamoto, *Infrared and Raman Spectra of Inorganic and Coordination Compounds* (Wiley–Interscience, New York, 1986) pp. 140, 329.
[19] F.D. Hardcastle and I.E. Wachs, J. Phys. Chem. 95 (1991) 5031.
[20] O.B. Lapina, B. Bal'zhinimaev, S. Boghosian, K.M. Eriksen and R. Fehrmann, Catal. Today (1997), in press.